Journal of Food Measurement and Characterization
https://doi.org/10.1007/s11694-026-04759-z

ORIGINAL PAPER

Biochemical and elemental composition stability of garlic (Allium sativum) under controlled 3.5 GHz radiofrequency exposure

Muhammad Zamir Mohyedin[1] · Aduwati Sali[1,2] · Nur Farah Afiqah Asmadi[1] · Nur Aisyah Malik[1] · Nurul Huda Abd Rahman[3] · Negin Foroughimehr[4,5] · Ali Yavari[4]

Received: 14 January 2026 / Accepted: 22 July 2026

Abstract

The rapid deployment of 5G-enabled smart farming infrastructure has increased the likelihood of continuous radiofrequency (RF) exposure of agricultural crops. However, standardized baseline data describing molecular and elemental stability of food crops under controlled 3.5 GHz RF exposure remain limited. In this study, a spectroscopy-based baseline assessment was conducted to evaluate the biochemical and elemental responses of garlic (Allium sativum) subjected to continuous-wave RF exposure at 3.5 GHz. Garlic cloves were exposed for 0 h (control), 2 h, 4 h, 6 h, and 8 h under controlled conditions within an anechoic chamber. Raman spectroscopy was employed to monitor molecular vibrational fingerprints, while X-ray fluorescence (XRF) was used to quantify major elemental constituents. Raman spectra revealed characteristic bands associated with organosulfur compounds, carbohydrates, and proteins, with no statistically significant deviations observed across exposure durations. Multivariate analysis using partial least squares demonstrated substantial overlap among all groups within the 95% Hotelling's T^2 confidence region, indicating preservation of baseline biochemical signatures. XRF analysis showed minor downward trends in magnesium, sulphur, chlorine, and potassium concentrations with increasing exposure duration. However, these observed fluctuations were not statistically significant and fell within baseline biological variability. These findings indicate that short-term continuous exposure to 3.5 GHz RF radiation for up to 8 h does not induce measurable deviations from baseline molecular or elemental variability in garlic. The results provide a reference benchmark for future investigations examining longer-term, cumulative, or field-scale RF exposure effects on agricultural crops.

Keywords Baseline assessment · 5G radiation · Radiofrequency exposure · Spectroscopic monitoring · Agricultural crop safety

✉ Muhammad Zamir Mohyedin
zamirmohyedin@upm.edu.my

✉ Aduwati Sali
aduwati@upm.edu.my

1 Institute for Mathematical Research (INSPEM), Universiti Putra Malaysia, Serdang 43400, Selangor, Malaysia

2 WiPNET Research Centre, Department of Computer and Communication Systems Engineering, Faculty of Engineering, Universiti Putra Malaysia (UPM), Serdang, Selangor, Malaysia

3 Microwave Research Institute (MRI), Universiti Teknologi MARA, Shah Alam 40450, Selangor, Malaysia

4 6G Research and Innovation Lab, Swinburne University of Technology, Melbourne, VIC 3122, Australia

5 Australian Synchrotron, Australian Nuclear Science & Technology Organisation, Melbourne, VIC 3168, Australia

Introduction

Smart farming technologies rely heavily on wireless communication to transmit data and control operations due to the wide and complex environment of agricultural fields. These technologies commonly use wireless communication systems such as LoRa, mobile broadband (e.g., 5G networks), Wi-Fi and Narrowband-IoT networks to enable real-time monitoring and management of crops and soil conditions [1–3]. Therefore, agricultural plants and soils are continuously subjected to radiofrequency (RF) electromagnetic exposure as an unintended consequence of smart farming infrastructure. This radiation occurs persistently in the field environment through overlapping signals from IoT nodes, drones, and mobile broadband towers [4, 5]. While these technologies are essential for data transmission and

Published online: 07 August 2026

automation, the constant exposure of RF radiation raises the need for systematic evaluation and baseline characterization of crop responses.

RF exposure has been reported to induce diverse responses in plants that range from harmful to beneficial. Some studies show negligible impact. RF radiation at 900 MHz has been shown to suppress root and shoot growth in *Vigna radiata* seedlings through oxidative stress pathways [6, 7]. Exposure of *Allium cepa* to 2,100-2,350 MHz resulted in genotoxic effects such as increased mitotic index and formation of laggard chromosomes [8, 9]. Similarly, *Arabidopsis thaliana* exposed to 2,450 MHz radiation has increased hydrogen peroxide and dehydroascorbic acid content which indicates activation of oxidative stress and a shift in cellular redox balance under RF exposure [10].

Conversely, certain exposures have been associated with beneficial effects such as enhanced germination rates and seedling growth in *Zea mays* seeds following 935–960 MHz exposure [11]. Exposure of *Withania somnifera* to 900 MHz radiation has increased phenolic compounds, flavonoid content and enhanced antioxidant activity [12]. Rice (*Oryza sativa L.*) was exposed to 2,450 MHz radiation has been reported to improved seed germination [13]. At the same time, several studies report no significant changes. Morphology, stem length and chlorophyll concentration of *Medicago sativa* undergoes no alteration when exposed to 2,400 MHz [14]. It is reported that 1,900 MHz radiation has no significant effect on gene activity in plant cells [15]. The wide range of reported outcomes highlights the absence of standardized baseline reference data under controlled RF exposure conditions, making cross-study comparison difficult.

Previous studies investigating RF–plant interactions have employed a wide range of experimental protocols, including different exposure frequencies, power levels, exposure durations, and biological models. Exposure intensities reported in the literature range from low environmental field strengths to higher laboratory-controlled levels, with exposure durations varying from minutes to several days. Moreover, experimental systems have examined whole plants, seedlings, germinating seeds, detached leaves, roots, or excised tissues, each of which may respond differently depending on developmental stage and tissue organization. Oxidative stress parameters, such as those measured in studies of chemical stressors in animal models [16], are established indicators of tissue degradation. Similar biochemical markers have been used to assess RF-induced plant responses, though such assays were beyond the scope of this baseline spectroscopic study. In this context, controlled baseline studies using clearly defined exposure parameters and sample configurations are essential. In the present work, intact garlic cloves were selected as a structurally and biochemically stable plant model. An exposure was conducted under controlled laboratory conditions with defined RF frequency, power level, and exposure duration.

In spite of extensive work across frequencies from hundreds of MHz to more than 2.4 GHz, there is a notable lack of studies specifically addressing 3.5 GHz which is the most commonly used frequency band in 5G networks [17, 18]. One of the primary operating frequencies for smart farming infrastructure is 3.5 GHz, providing internet connectivity for IoT devices, wireless sensors and autonomous agricultural machinery [19–21]. Before mechanistic or long-term biological effects can be meaningfully interpreted, baseline molecular and elemental stability under this frequency must first be established.

Therefore, garlic (Allium sativum), as a widely consumed staple crop with well-characterized biochemical and elemental composition, provides a suitable model system for baseline spectroscopic assessment. To the best of our knowledge, no studies to date have reported baseline molecular and elemental responses of garlic under controlled 3.5 GHz RF radiation exposure. Previous investigations have predominantly relied on growth-based or biochemical assays, highlighting the need for standardized spectroscopic reference data under defined exposure conditions [22, 23]. This is particularly relevant as various non-thermal physical treatments are increasingly being explored for modern post-harvest and smart agricultural applications, making baseline compositional stability data essential for distinguishing external treatment effects from natural biological variability.

Most prior RF–plant studies have relied on growth metrics, physiological indicators or targeted biochemical assays, which can be sensitive to experimental variability and may not provide direct insight into underlying molecular and elemental stability. In contrast, spectroscopic techniques offer non-destructive, label-free assessment of intrinsic molecular and elemental composition. Raman spectroscopy enables direct probing of molecular vibrational signatures associated with key biochemical constituents, while X-ray fluorescence (XRF) provides complementary information on elemental composition without extensive sample preparation. The combination of vibrational and elemental spectroscopy with multivariate analysis has been successfully applied to assess material stability under various stressors [24], supporting our approach for RF-exposed plant tissues. Together, these techniques are well suited for establishing baseline molecular and elemental reference data under controlled RF exposure conditions.

In this work, we employ a spectroscopy-based approach combining Raman spectroscopy for molecular vibrational profiling and XRF for elemental quantification to establish baseline molecular and elemental stability under controlled RF exposure conditions. Raman spectroscopy has been

widely applied to assess nutrient distribution, stress-related signatures, and biochemical composition in plant tissues [25–27]. XRF, on the other hand, has been employed for non-destructive quantification of mineral nutrients and trace elements in plant tissues [28, 29].

The objective of this study was to establish a spectroscopy-based baseline assessment of molecular and elemental stability in garlic subjected to continuous 3.5 GHz RF exposure under controlled conditions. Raman spectroscopy was employed to monitor biochemical fingerprints, while X-ray fluorescence was used to quantify elemental composition across increasing exposure durations. Rather than probing specific biological mechanisms, this work provides a reference benchmark against which future long-term, cumulative or field-scale RF exposure studies may be evaluated.

Methodology

This study was designed to establish baseline biochemical and elemental responses in garlic following controlled exposure to radiofrequency (RF) radiation at 3.5 GHz. The methodology consisted of four major components: (i) sample preparation, (ii) RF radiation exposure using a signal generator and horn antenna within an anechoic chamber, (iii) biochemical profiling of garlic tissue using Raman spectroscopy, and (iv) elemental profiling using X-ray fluorescence (XRF) analysis.

Sample preparation

Fresh garlic cloves (*Allium sativum*) were obtained from a local supermarket. To minimize variability, all samples were procured on the same day from the same batch. The outer dry skin of each garlic bulb was removed, and individual cloves were separated and peeled.

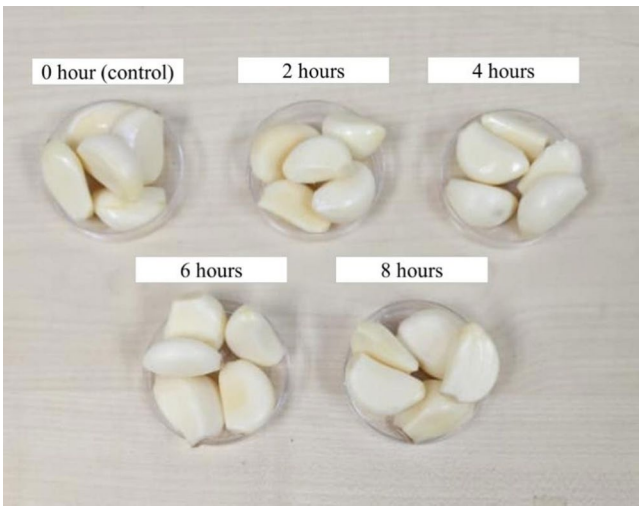

Fig. 1 Garlic cloves assigned to the control (0 h) and RF exposure groups (2 h, 4 h, 6 h and 8 h). Each group consisted of five biological replicates placed individually in petri dishes

To ensure consistency and minimize allocation bias, a constrained randomized design was applied. Only cloves with masses between 5 and 7 g were selected to reduce variability associated with sample size. Eligible cloves were randomly assigned to control (no RF exposure), 2 h, 4 h, 6 h and 8 h exposure groups as illustrated in Fig. 1. Each group consisted of five biological replicates. All cloves were placed individually in petri dishes to prevent cross-contamination and to ensure uniform exposure conditions across samples. Five biological replicates per exposure group were selected to establish baseline molecular and elemental variability under controlled RF exposure conditions, consistent with exploratory spectroscopic studies where the objective is to assess stability rather than to detect subtle effect sizes. We acknowledge that a sample size of ($n=5$) limits statistical power. Given the inherent heterogeneity of plant tissues, a larger sample size ($n \geq 6$–8) is generally preferred to capture broader biological variations, and this lower sample count represents a limitation of the current baseline study.

Radiofrequency exposure protocol

RF exposure was performed using a N5173B EXG Analog Signal Generator (Keysight Technologies, Santa Rosa, California) that connected to a LB-81,810-NF broadband horn antenna (A-INFO, Irvine, California) as shown in Fig. 2. The signal generator was calibrated prior to the experiment to ensure a stable output of 3.5 GHz at 10 dBm in continuous-wave mode.

Garlic samples were placed in Petri dishes and positioned 20 cm below the horn antenna aperture, with the sample surface oriented vertically toward the antenna aperture, as shown in Fig. 3. This distance corresponds to approximately 2.3 wavelengths at 3.5 GHz ($\lambda \approx 8.6$ cm), placing the samples outside the reactive near-field region of the antenna, where the electromagnetic field distribution is more stable and spatially uniform. Temperature was not actively monitored during exposure. However, given that the exposure setup maintained a continuous-wave RF field strength at an estimated 9.4 V/m (equivalent to an incident power density of approximately 0.234 W/m^2), this energy levels fall well below the thresholds required to induce significant dielectric heating in high-water-content biological tissues, operating under a strictly non-thermal exposure framework over the 8 h window [30]. The setup was enclosed within a shielded anechoic chamber to minimize external electromagnetic interference and unwanted reflections. Control samples were kept in a Faraday-shielded container prior to exposure to minimize any unintentional RF exposure from the environment.

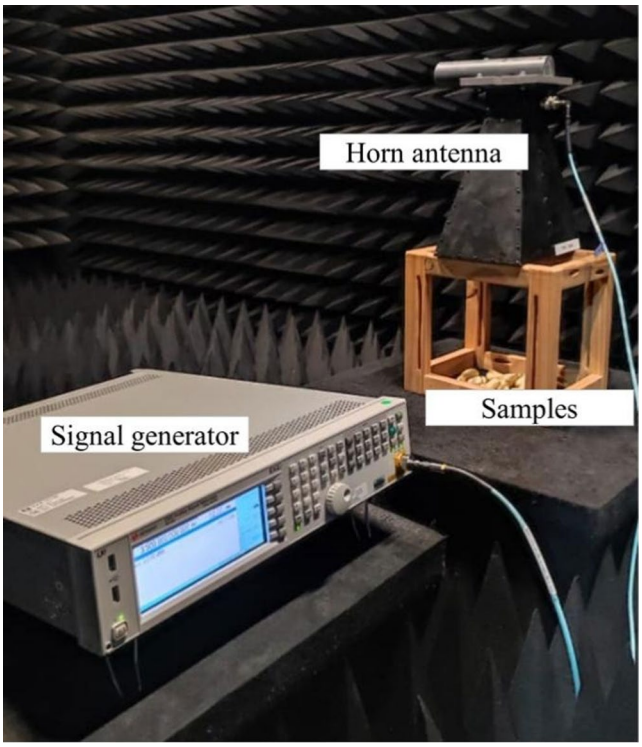

Fig. 2 Experimental setup of the RF exposure system, comprising a signal generator connected to a horn antenna inside an anechoic chamber operating at 3.5 GHz

The exposure protocol consisted of five treatment groups which were control, 2 h, 4 h, 6 h and 8 h with each comprising five biological replicates. During the experiment, the exposure was applied continuously. At each time point, the corresponding samples were removed from the exposure chamber and immediately transferred to the Faraday box to prevent further exposure. Specifically, samples assigned to the 2 h group were taken out after 2 h, followed by removal of the 4 h, 6 h and 8 h groups at their respective endpoints. All samples were handled consistently to minimize variability due to handling and environmental factors, ensuring that the only difference between groups was the exposure duration.

Raman spectroscopy analysis

Raman measurement was performed on a WITec Alpha 300R confocal microscope system (Oxford Instruments, Ulm, Germany). Excitation was provided by 532 nm laser, dispersed by a T1 grating of 600 g/mm and blazed diffraction grating of 500 nm with the spectrograph centered at 1996.8 cm^{-1}. Spectra were acquired over 101 cm^{-1} to 3100 cm^{-1} with an integration of 5.065 s per spectrum. However, 400 cm^{-1} to 2000 cm^{-1} region was selected as the relevant biochemical fingerprint range [31].

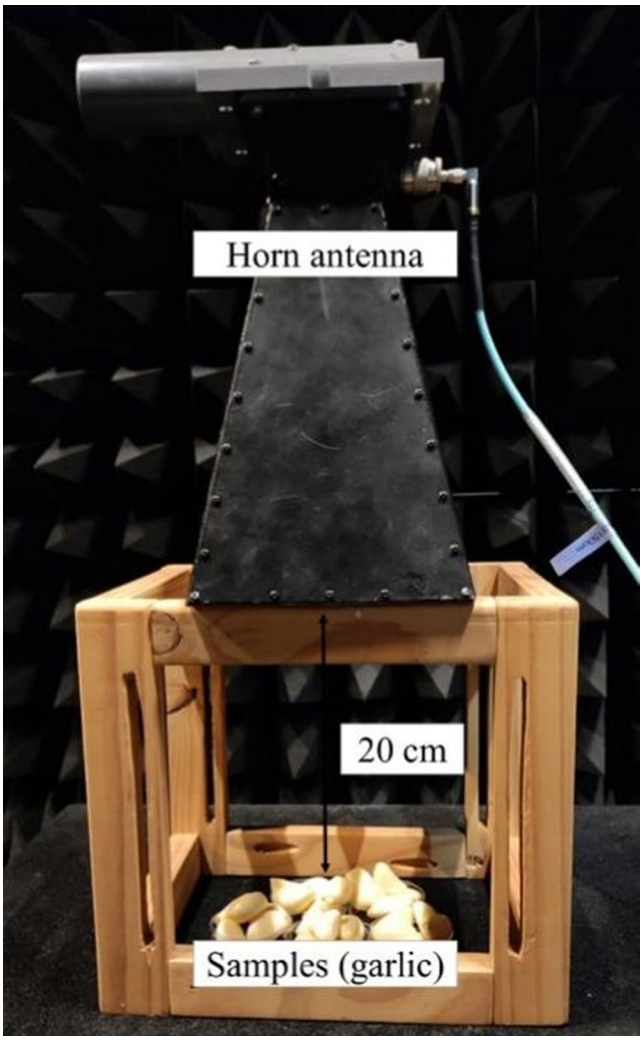

Fig. 3 Experimental arrangement of garlic samples placed directly beneath the horn antenna within the anechoic chamber

Garlic cloves were sliced into a 2–3 mm thickness and measured directly under the Raman microscope. Spectra were acquired from the brownish white tissue region of each clove as shown in Fig. 4, while the central clear white region was consistently avoided. Spectrum was collected per clove, thus there are five replicates for each group.

Statistical analysis

Prior to statistical analysis, the Raman spectra were processed by baseline correction using asymmetric least-squares (ALS) algorithm. This approach was chosen because ALS effectively removes sloping or curved backgrounds caused by scattering or instrumental effects, while preserving sharp spectral peaks. Corrected spectra were then normalized to the 1460 cm^{-1} band as recommended in the literature for plant matrices [32]. Subsequently, Partial

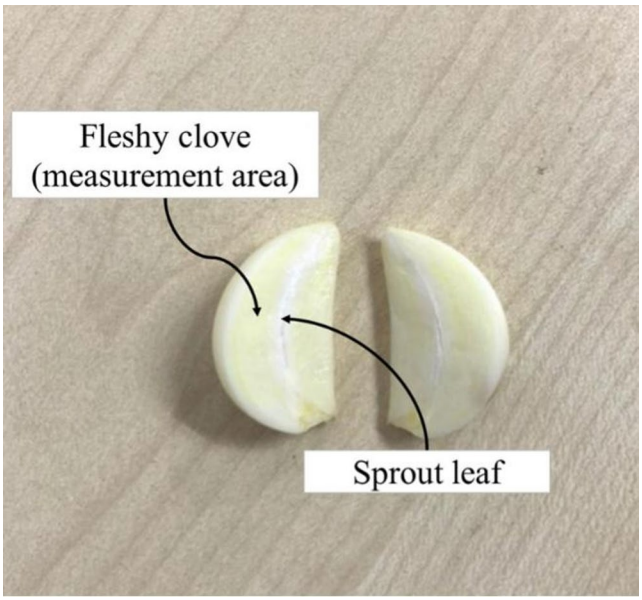

Fig. 4 Garlic clove cross-section indicating the sprout leaf and measurement area at the fleshy clove

Least Squares (PLS) analysis was performed using singular value decomposition (SVD) algorithm with a maximum of 15 factors [33]. The raw data of the Raman spectra for the PLS analysis has been made available [34]. The optimal number of factors was auto determined automatically by Origin software using a leave-one-out cross-validation method [35, 36]. Model validation employed the cross-validation procedure. Peak parameters were analysed with Kruskal–Wallis ANOVA with Dunn's test applied for post-hoc multiple comparisons [37–39].

Statistical analyses were performed using non-parametric methods due to the limited sample size and the absence of normality assumptions for spectroscopic intensity data. The Kruskal–Wallis test was used to compare Raman band intensities and elemental concentrations across exposure groups, followed by Dunn's post-hoc test for pairwise comparisons where applicable. Effect sizes (η^2) were calculated to assess the magnitude of differences independent of statistical significance. This approach is appropriate for exploratory baseline studies and reduces the risk of false-positive conclusions when sample sizes are modest.

All Raman spectra were baseline-corrected to remove fluorescence and background contributions using identical preprocessing parameters for all samples. Background intensity levels were examined to verify that no systematic increase occurred with increasing RF exposure duration.

X-ray fluorescence (XRF) analysis

Elemental analysis was performed using an Epsilon 3-XL energy-dispersive X-ray fluorescence spectrometer (Malvern Panalytical, Malvern, United Kingdom) equipped with a silicon drift detector (SDD) and measurements were conducted under air atmosphere. The instrument was configured to detect major nutrient elements relevant to garlic tissue including sulphur (S), phosphorus (P), potassium (K), magnesium (Mg) and chlorine (Cl).

For sample preparation, multiple garlic cloves with a total weight of approximately 25 g from each treatment group were exposed to RF as described in Sect. 2.2. Following exposure, samples were sliced and dried at 60 °C for 24 h which reducing the mass of the samples to ~10 g. The dried tissue was ground into a fine powder. Approximately 10 g of powdered garlic was loaded into XRF sample cup and sealed with a thin Mylar film to contain the powder while allowing X-rays to pass through without significant interference, as well as to provide a chemically inert and stable barrier during measurement.

Each sample was scanned three times to account for instrumental variability. Spectral deconvolution and quantification were performed using the Epsilon 3 software. Elemental concentrations were reported as atomic percentages (%). Calibration of the instrument was performed using Standard Reference Materials (SRM) which are samples with certified elemental compositions, to ensure accurate and reliable quantification [40]. All measurements were carried out under consistent instrumental settings and environmental conditions to minimize additional sources of variability.

Results

This study assessed molecular and elemental stability in garlic (Allium sativum) under continuous-wave 3.5 GHz RF radiation exposure at different durations, namely 0 h, 2 h, 4 h, 6 h, and 8 h. Raman spectroscopy was employed to characterize vibrational fingerprints associated with major biochemical components. Partial Least Squares (PLS) analysis was used to evaluate overall spectral variation across groups. Elemental profiling was performed using X-ray fluorescence (XRF) to evaluate mineral composition across exposure durations.

Result of raman analysis

Figure 5 shows the averaged Raman spectra of garlic cloves exposed to 3.5 GHz RF radiation at different durations (0–8 h). Across all groups, the spectra exhibit similar profiles, with several characteristic vibrational bands evident as tabulated in Table 1. The observed Raman spectral features are consistent with those previously reported for garlic in the literature [31, 41, 42].

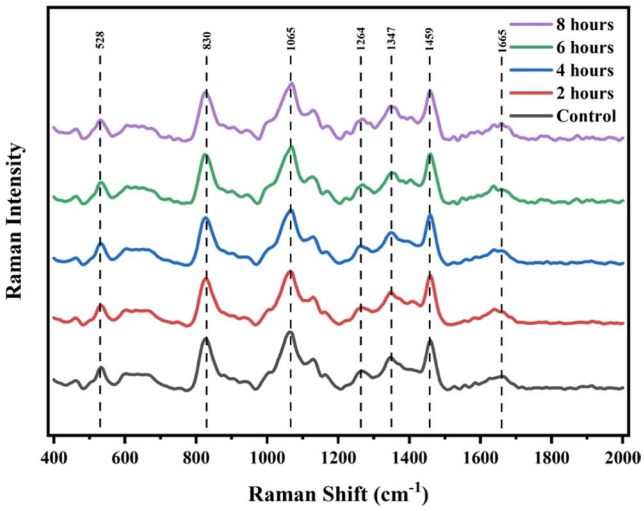

Fig. 5 Raman spectra of garlic samples across different RF exposure durations (control, 2 h, 4 h, 6 h, and 8 h)

Table 1 Major Raman band and its corresponding substance in the garlic

Raman Shift (cm^{-1})	Vibrational Mode	Biochemical assignment	References
528	S-S stretching	Disulfide	[43–45]
830	C-C stretching	Proline-related vibration	[46]
1065	Skeletal C-O stretching Skeletal C-C stretching	Pectic acid vibration	[31]
1264	C-N stretching N-H bending	Amide III (protein backbone)	[42, 46]
1347	C-C stretching C-H bending	Carotene-related vibration	[31]
1459	CH_2 bending (deformation)	Methylene deformation	[31]
1665	C = O stretching	Amide I (C = O stretching)	[31, 46]

Overall, the spectral profiles remained broadly consistent across control and radiation-exposed groups. Minor visual variations were observed in the positions and relative intensities of certain bands, particularly near 1065 cm^{-1} and 1264 cm^{-1}, as well as weak shoulder features around approximately 1225 cm^{-1} and 1425 cm^{-1} in the stacked spectra. Flavonoid-related bands in the 1200–1600 cm^{-1} region have been previously reported in bulb tissues [47], consistent with the 1347 cm^{-1} and 1459 cm^{-1} bands observed here. However, these variations did not exhibit a systematic shift with increasing exposure duration and remained within baseline spectral variability. The intensity differences between groups were also within baseline variability. Statistical comparison of normalized Raman intensities at major vibrational bands (528 cm^{-1}, 830 cm^{-1}, 1065 cm^{-1}, 1264 cm^{-1}, 1347 cm^{-1}, and 1665 cm^{-1}) was performed using the Kruskal–Wallis test followed by Dunn's post-hoc analysis. Individual Kruskal-Wallis tests conducted on each major vibrational band revealed no significant differences among the control and exposed groups at the $\alpha = 0.05$ level. Each evaluated band independently yielded an identical chi-square value of $\chi^2 = 4$ and an identical asymptotic p-value of $p = 0.406$), confirming that the median peak intensities were statistically indistinguishable among all exposure groups at each of the selected wavenumbers (528 cm^{-1}, 830 cm^{-1}, 1065 cm^{-1}, 1264 cm^{-1}, 1347 cm^{-1}, and 1665 cm^{-1}). The effect size (η^2) for the Kruskal–Wallis tests at all major Raman bands was < 0.01, indicating negligible differences and preservation of baseline spectral characteristics. The normalized Raman intensities at the major vibrational bands (528 cm^{-1}, 830 cm^{-1}, 1065 cm^{-1}, 1264 cm^{-1}, 1347 cm^{-1}, and 1665 cm^{-1}) showed low variability within each exposure group, with standard deviations between 0.0446 and 0.0713. This supports the conclusion that the observed spectral profiles remained within baseline variability under the applied RF exposure conditions.

Inspection of the baseline-corrected spectra showed no systematic increase in background intensity or fluorescence contribution with increasing RF exposure duration, indicating that background effects did not dominate the observed Raman features. These results indicate that the spectral features associated with major biochemical constituents of garlic remained consistent across exposure durations. Furthermore, statistical analysis showed that the intensity of individual Raman bands remained within baseline variability across all exposure durations under the experimental conditions.

To assess collective spectral variation across exposure groups, Partial Least Squares (PLS) regression was applied. PLS was selected because it is well suited for spectral datasets, which are often high-dimensional and contain strongly correlated variables. By projecting the spectra into latent factors that capture the dominant variance structure, PLS facilitates visualization of multivariate patterns that may not be apparent in the raw data. Figure 6 shows the PLS score plot for the first two latent factors. The plot shows that spectra from control and exposed groups largely overlap, with no clear separation between groups. The 95% Hotelling's T^2 ellipse represents a multivariate confidence region, defining the statistical boundary within which approximately 95% of samples are expected to fall if they originate from the same population [48]. All Raman spectra in this study fell within this region, confirming the absence of multivariate outliers. The observed multivariate variation between control and exposed groups was minimal and remained within the baseline confidence region.

However, a weak displacement along Factor 1 was observed, with several spectra from the 6 h and 8 h exposure

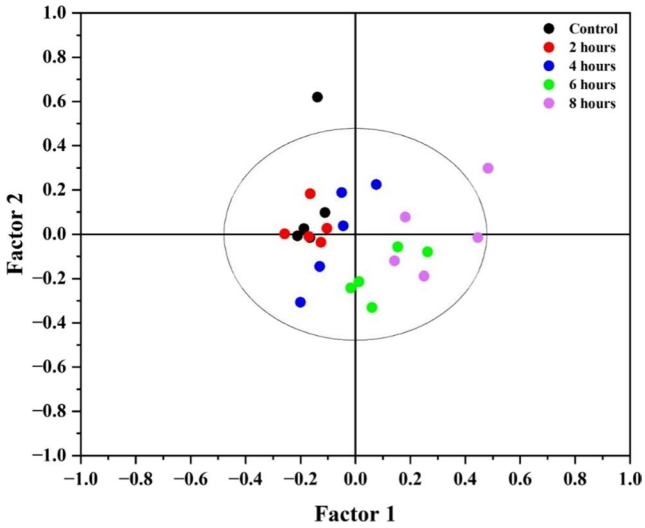

Fig. 6 Partial Least Squares (PLS) score plot of garlic samples across different RF exposure durations (control, 2 h, 4 h, 6 h, and 8 h) projected onto Factor 1 and Factor 2

groups shifted slightly toward positive scores. Meanwhile, some spectra from the 6 h exposure group were distributed toward negative scores along the same axis. The 2 h and 4 h exposure groups remained distributed closer to the control group. Although this pattern reflects minor multivariate displacement at longer exposure durations, the degree of overlap within the Hotelling's T^2 confidence ellipse indicates that these variations remain within baseline confidence limits and are not strongly discriminating between groups.

PLS analysis showed that Raman spectra of garlic remained within baseline multivariate variability across RF exposure durations up to 8 h, with no major deviations observed, although minor collective multivariate displacement was present.

Result of X-ray fluorescence (XRF) analysis

XRF analysis was conducted to assess the elemental composition of garlic across exposure durations. The concentrations of four major elements which are magnesium (Mg), sulphur (S), chlorine (Cl) and potassium (K) are presented in Fig. 7. The error bars represent a ± 5% relative uncertainty of the measured elemental concentrations, reflecting analytical measurement error rather than biological variation.

The elemental concentrations exhibited modest variation across exposure durations. Magnesium remained relatively stable from 0 h to 6 h with concentrations around 0.1%, and was lower at 8 h (0.08%). Concentrations of sulphur, a key component of organosulfur compounds, ranged from approximately 1.5% at 0 h to 1.0% at 8 h. Similar variations were observed for chlorine and potassium across exposure groups, with potassium concentrations ranging from 5.2% at 0 h to 3.8% at 8 h. Although the samples were analysed in dried powder form, the absolute elemental percentages differ

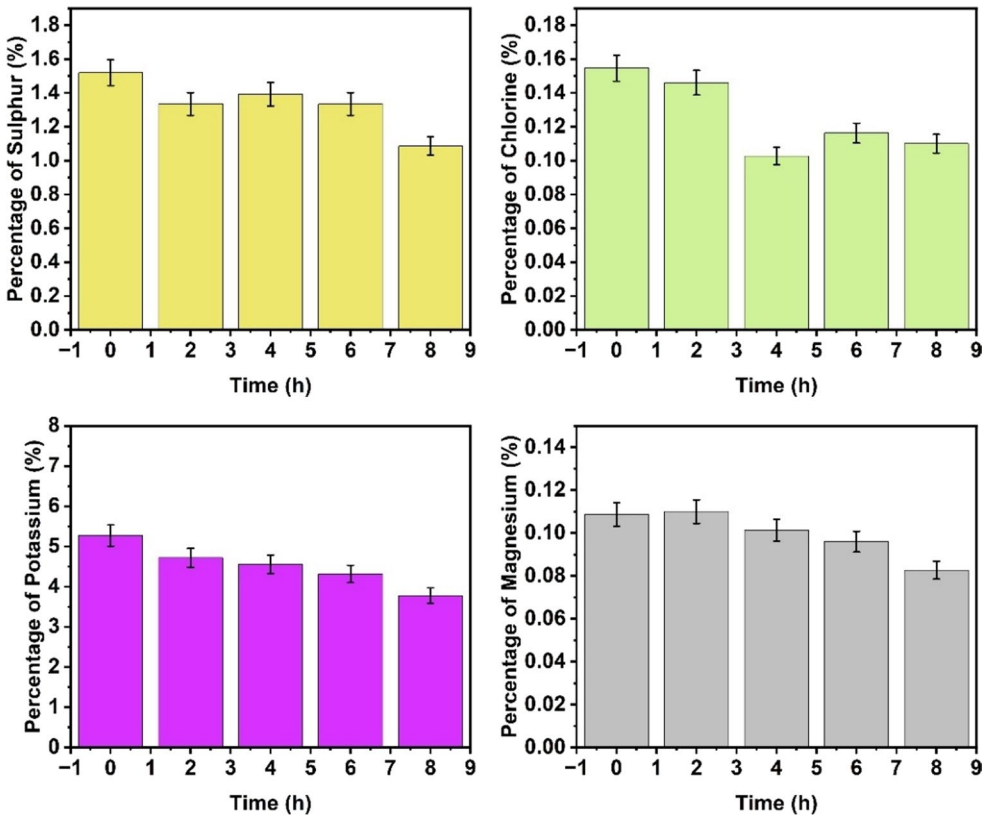

Fig. 7 Changes in atomic percentage of sulphur (S), chlorine (Cl), potassium (K) and magnesium (Mg) in garlic samples across RF exposure times

from values reported in the literature, which is expected due to differences in analytical methodology. Most reported garlic elemental compositions are obtained using digestion-based techniques such as ICP-OES or ICP-MS, whereas the present study employed semi-quantitative XRF analysis, which is sensitive to matrix effects, particle size, and sample density. Nevertheless, the relative abundance and ordering of the major elements (K > S > Cl > Mg) are consistent with previously reported garlic compositions, supporting the reliability of the measurements [49–51].

Although modest reductions in absolute values were observed, statistical analysis using the Kruskal–Wallis test confirmed no significant differences in elemental concentrations among control and exposed groups for all measured elements ($p > 0.05$). Within the 8 h exposure window, the elemental composition of garlic remained within baseline variability.

Discussion

This study aimed to establish baseline molecular and elemental stability in garlic under controlled 3.5 GHz continuous-wave RF exposure using a dual-spectroscopy approach. Raman spectroscopy showed that molecular vibrational fingerprints associated with major biochemical components remained within baseline variability across exposure durations up to 8 h, with multivariate analysis indicating minimal variation.

The Raman analysis indicates that the molecular spectral features of garlic remained stable within the baseline range under the tested exposure conditions. Previous studies on plant systems have reported a wide range of responses to electromagnetic exposure, including beneficial, adverse, and negligible effects, depending on frequency, exposure duration, and tissue type [22, 23]. A subset of studies has similarly reported negligible responses, consistent with the baseline stability observed in the present study [15, 52]. One hypothetical contributing factor may relate to the penetration characteristics of the applied frequency. The 3.5 GHz band, while relevant to 5G communication, exhibits a shorter wavelength and reduced penetration depth compared to lower frequencies such as 900 MHz or 2.45 GHz commonly used in earlier plant exposure studies. Consequently, it can be hypothesized that a larger proportion of the electromagnetic energy may be confined to surface regions, potentially limiting interaction with inner tissues where Raman measurements were obtained. This consideration may partly explain the minimal multivariate variation observed. In contrast to pulsed electric fields, which directly disrupt cell membranes [53], the continuous-wave RF exposure used here operates at non-thermal power levels unlikely to cause similar structural effects. However, this interpretation is presented as a qualitative consideration, and further work incorporating field distribution measurements would be required to substantiate this effect.

Additionally, no noticeable shifts or intensity changes were observed in the Raman peaks corresponding to disulfide (528 cm^{-1}), proline (830 cm^{-1}), pectic acid (1065 cm^{-1}), amide III (1264 cm^{-1}), carotene (1347 cm^{-1}), methylene (1459 cm^{-1}), and amide I (1665 cm^{-1}). The observed spectral stability is consistent with preservation of molecular features associated with these functional groups under the tested exposure conditions. Analogous to high-intensity pulsed magnetic fields, which preserve primary molecular structure while affecting higher-order interactions [54], the RF exposure in this study did not alter the fundamental vibrational fingerprints of garlic biomolecules. In Raman spectroscopy, peak position and intensity are sensitive indicators of bond stretching, bending, or disruption [55, 56]. Accordingly, the absence of detectable variation suggests that the disulfide (S–S), C–H, C–C and C = O bonds did not show evidence of disruption within the sensitivity limits of the Raman measurements. Similar to ultrasound-assisted extraction, which preserves molecular structure while enhancing release [57], the RF exposure in this study did not induce detectable bond disruptions in organosulfur compounds. The lack of detectable Raman peak shifts, which would otherwise indicate structural or conformational alterations under external stress, further supports the fundamental molecular stability of the RF-exposed garlic tissues. This observation is consistent with the non-ionizing and low-energy nature of RF exposure in the GHz range, which is generally insufficient to directly induce chemical bond breakage under short-term exposure conditions.

The XRF results shown in Fig. 7 indicate that the elemental concentrations of magnesium, sulphur, chlorine, and potassium exhibited a slight decreasing trend with increasing exposure duration. The absolute reductions across all measured elements were within 1.5% points. Given that these minor shifts did not achieve statistical significance ($p > 0.05$), they can be considered to fall within the baseline variability expected from natural biological heterogeneity or hydration-related differences commonly present in plant tissues. Nevertheless, the modest downward trend observed at longer exposure durations (6 h and 8 h) highlights a pattern that may warrant closer examination in future studies employing extended exposure times.

Sulphur and potassium are particularly important elements due to their central roles in garlic chemistry and physiology. Sulphur is a key component of organosulfur compounds such as alliin and allicin, which contribute to garlic's characteristic bioactivity and nutritional value [58, 59]. However, given the exploratory sample size ($n = 5$) and

the inherent biological variance of plant tissue, the statistical framework possesses a large Minimum Detectable Difference (MDD). Due to high MDD limits the power of the Kruskal–Wallis test to detect anything short of massive variations, the observed descriptive decrease in sulphur from 1.5% to 1.0% (approximately 33.3% relative reduction) could be highly meaningful biologically due to its central role in allicin chemistry, despite lacking statistical significance here. This suggests that the observed downward trend should not be dismissed as mere baseline noise, but rather highlights a potential biological response that warrants targeted verification with larger sample sizes.

Additionally, to prepare the samples for semi-quantitative XRF analysis, an oven-drying protocol (60 °C for 24 h) was utilized to halt biological activity, standardize moisture content, and stabilize the tissue matrix into a grindable powder form [60]. While thermal drying is a standard method to lock the elemental profile of plant tissues post-exposure, we acknowledge that high-temperature processing can volatilize volatile organosulphur compounds [61, 62]. While any sulphur loss from the oven heat should happen equally to all groups, it is theoretically possible that the RF exposure made the sulfur compounds in the treated garlic more sensitive to heat evaporation. This remains a minor limitation of using dried samples, and future studies using fresh, non-destructive methods will be needed to completely separate the effects of radiation from the effects of oven drying.

Potassium is an essential macronutrient influencing plant growth, yield, and cellular osmotic regulation [63, 64]. Even subtle variations in these elements may be relevant for future investigations examining biochemical responses under prolonged RF exposure [65, 66]. Future studies with extended exposure durations will be required to determine whether such variations develop into biologically meaningful effects. Future studies also should consider whether prolonged RF exposure could influence iron-mediated oxidative pathways, as iron-dependent processes such as ferroptosis are sensitive to subtle changes in redox balance. In addition, advanced techniques such as synchrotron-based X-ray absorption spectroscopy (XAS) in the tender energy range could provide detailed information on sulphur speciation in garlic, enabling detection of changes in oxidation state or bonding environment. Such approaches may help clarify whether 3.5 GHz RF exposure is associated with changes in sulphur chemical forms and how these relate to garlic physiology and nutritional quality.

Furthermore, the RF exposure level used in this study corresponds to an estimated electric field strength of approximately 9.4 V/m, which is well below the ICNIRP reference level for general public exposure at 3.5 GHz (~61 V/m). This contextualizes the exposure conditions within commonly encountered environmental and smart-farming RF levels. It should be noted that compliance with ICNIRP reference levels does not preclude subtle biological responses. However, within the tested exposure window, molecular and elemental parameters remained within baseline variability.

Conclusion

In summary, this study established baseline molecular and elemental responses of garlic under controlled 3.5 GHz continuous-wave RF exposure using a dual-spectroscopy approach. Raman spectroscopy showed that molecular vibrational fingerprints associated with major biochemical components remained within baseline variability across exposure durations up to 8 h, with multivariate analysis indicating minimal spectral variation. Complementary XRF analysis revealed modest decreases in elemental concentrations of Mg, S, Cl, and K. However, the magnitude of change was less than 5% and remained statistically non-significant across the measured exposure window. Collectively, these findings indicate that short-term exposure to 3.5 GHz RF radiation under the tested conditions is associated with preserved molecular and elemental stability in garlic. The modest trends observed at longer exposure durations highlight patterns that may warrant further investigation in studies incorporating extended exposure periods or additional analytical endpoints. Future work expanding exposure duration and experimental scope will be valuable for contextualizing RF interactions with agricultural crops in smart farming environments.

Acknowledgements This work was supported by Universiti Putra Malaysia (UPM) under Geran Putra Berimpak [grant number GBP/2024/9783500]. The authors gratefully acknowledge Universiti Teknologi MARA (UiTM) for the facilities provided. The authors also acknowledge the BioEM Society for support under the Short-Term Mission 2025, which facilitated the acquisition of essential skills to carry out this work.

Author contributions Muhammad Zamir Mohyedin contributed to the conceptualization, methodology design, data analysis, visualization and manuscript drafting. Nurul Huda Abd Rahman, Nur Aisyah Malik and Nur Farah Afiqah Asmadi contributed to resources, data curation, and methodology. Negin Foroughimehr contributed to validation and manuscript revision. Aduwati Sali and Ali Yavari contributed to supervision, validation, project administration, and funding acquisition. All authors reviewed and approved the final version of the manuscript.

Funding Open access funding provided by The Ministry of Higher Education Malaysia and Universiti Putra Malaysia

Data availability The raw data for the Raman analysis and PLS analysis are available at Mohyedin, Muhammad Zamir (2025), "Garlic Raman Spectra (Raw Data) for PLS Analysis", Mendeley Data, V1, doi: https://doi.org/10.17632/9h76kntxr5.1.

Declarations

Competing interest The authors declare that they have no known competing financial interests or personal relationships that could have appeared to influence the work reported in this paper.

References

1. L. Aldhaheri, N. Alshehhi, I.I.J. Manzil, R.A. Khalil, S. Javaid, N. Saeed, M.-S. Alouini, IEEE Internet Things J. **12**(2), 1380–1407 (2024)
2. M.N. Mowla, N. Mowla, A.F.M.S. Shah, K.M. Rabie, T. Shongwe, IEEe Access. **11**, 145813 (2023)
3. N.F.A. Asmadi, A. Sali, N.H. Abd Rahman, S. Paiman, M.Z. Mohyedin, Progress Electromagnet. Res. C **161**, 150–158 (2025)
4. P. Ruijie, A. Sali, L. Li, M.Z. Mohyedin, S. Qahtan, IEEE Access (2025)
5. I. Tahir, A. Sali, S.Q. Wali, A. Ismail, D. Suka, M.Z. Mohyedin, Progress Electromagnet. Res. C **156**, 93–100 (2025)
6. H.P. Singh, V.P. Sharma, D.R. Batish, R.K. Kohli, Environ. Monit. Assess. **184**, 1813 (2012)
7. V.P. Sharma, H.P. Singh, D.R. Batish, R.K. Kohli, Z. Für Naturforschung C **65**, 66 (2010)
8. S. Chandel, S. Kaur, M. Issa, H.P. Singh, D.R. Batish, R.K. Kohli, Protoplasma. **256**, 1399 (2019)
9. S. Chandel, S. Kaur, M. Issa, H.P. Singh, D.R. Batish, R.K. Kohli, J. Environ. Health Sci. Eng. **17**, 97 (2019)
10. A. Porcher, S. Girard, P. Bonnet, R. Rouveure, V. Guérin, F. Paladian, A. Vian, J. Plant. Physiol. **286**, 153999 (2023)
11. A.A. Khalafallah, S.M. Sallam, Romanian J. Biophys. **19**, 49 (2009)
12. C. Upadhyaya, I. Patel, T. Upadhyaya, A. Desai, in *Inventive Systems and Control: Proceedings of ICISC 2021*Springer, (2021), pp. 951–964
13. D. Talei, A. Valdiani, M. Maziah, M. Mohsenkhah, The Scientific World Journal 2013, 408026 (2013)
14. J.W. Skiles, Acta Astronaut. **58**, 258 (2006)
15. J.C. Engelmann, R. Deeken, T. Müller, G. Nimtz, M.R.G. Roelfsema, R. Hedrich, Adv. Appl. Bioinf. Chem. **1**, 71–83 (2008)
16. W. Ma, S. Wei, W. Peng, T. Sun, J. Huang, R. Yu, B. Zhang, W. Li, Biomed Res. Int. 2021, 6688855 (2021)
17. J. Lun, P. Frenger, A. Furuskar, E. Trojer, in *2019 IEEE 90th Vehicular Technology Conference (VTC*2019*-Fall)* (IEEE, 2019), pp. 1–6
18. G.S.M.A. Intelligence, *3.5 GHz in the 5G Era: Preparing for New Services in 3.3–4.2 GHz* (2021)
19. M. Van Hilten, S. Wolfert, Comput. Electron. Agric. **201**, 107291 (2022)
20. W. Arrubla-Hoyos, A. Ojeda-Beltrán, A. Solano-Barliza, G. Rambauth-Ibarra, A. Barrios-Ulloa, D. Cama-Pinto, F.M. Arrabal-Campos, J.A. Martínez-Lao, A. Cama-Pinto, and F. Manzano-Agugliaro, Sensors 22, 7295 (2022)
21. L. Vassiliou, A. Nadeem, D. Chatzichristodoulou, P. Vryonides, S. Nikolaou, Sensors. **24**, 3465 (2024)
22. D.K. Panda, D.P. Das, S.K. Behera, N.K. Dhal, Environ. Monit. Assess. **196**, 565 (2024)
23. M.N. Halgamuge, Electromagn. Biol. Med. **36**, 213 (2017)
24. L. Jia, P. Du, Z. Wang, Q. Duan, Y. Zhang, S. Hou, R. Ma, L. Zhao, R. Nie, S. Jia, Adv. Funct. Mater. **36**, e31648 (2026)
25. N. Altangerel, G.O. Ariunbold, C. Gorman, M.H. Alkahtani, E.J. Borrego, D. Bohlmeyer, P. Hemmer, M.V. Kolomiets, J.S. Yuan, M.O. Scully, Proceedings of the National Academy of Sciences 114, 3393 (2017)
26. W.Z. Payne, D. Kurouski, Front. Plant. Sci. **11**, 616672 (2021)
27. M. Roy, A. Prasad, Mater. (Oxf). **24**, 101474 (2022)
28. E.S. Rodrigues, M.H.F. Gomes, N.M. Duran, J.G.B. Cassanji, T.N.M. da Cruz, A. Sant'Anna, S.M. Neto, E. Savassa, de Almeida, W. P. Carvalho, Front. Plant. Sci. **9**, 1588 (2018)
29. G.S. Montanha, E.S. Rodrigues, J.P.R. Marques, E. De Almeida, A.R. Dos, Reis, and H. W. Pereira de Carvalho, Metallomics 12, 183 (2020)
30. D. Colombi, B. Xu, D. Anguiano Sanjurjo, P. Joshi, F. Ghasemifard, C. Di Paola, C. Törnevik, Front. Commun. Networks. **3**, 744528 (2022)
31. S. Vuković, Đ. Moravčević, J. Gvozdanović-Varga, A.Ž. Kostić, A. Vujošević, S. Kilibarda, I. Pećinar, in *Biology and Life Sciences Forum*MDPI, (2022), p. 21
32. W.Z. Payne, D. Kurouski, Plant. Methods. **17**, 78 (2021)
33. H. Abdi, Encyclopedia Meas. Stat. **907**, 44 (2007)
34. M.Z. Mohyedin, (2025)
35. T.-T. Wong, Pattern Recognit. **48**, 2839 (2015)
36. N. Zhao, Z. Wu, Q. Zhang, X. Shi, Q. Ma, Y. Qiao, Sci. Rep. **5**, 11647 (2015)
37. P.E. McKight, J. Najab, Corsini Encyclopedia Psychol. **1**, 1 (2010)
38. E. Ostertagova, O. Ostertag, J. Kováč, Appl. Mech. Mater. **611**, 115 (2014)
39. A. Dinno, Stata J. **15**, 292 (2015)
40. G.Y. Tao, Z.Y. Zhang, A. Ji, X-Ray Spectrom. **19**, 85 (1990)
41. X. Lu, B.A. Rasco, J.M.F. Jabal, D.E. Aston, M. Lin, M.E. Konkel, Appl. Environ. Microbiol. **77**, 5257 (2011)
42. Z. Wang, C. Li, Z. Wang, Y. Li, B. Hu, Vib. Spectrosc. **125**, 103509 (2023)
43. F. Adar, (2022)
44. B. Hernández, F. Pflüger, E. López-Tobar, S.G. Kruglik, J.V. Garcia-Ramos, S. Sanchez-Cortes, M. Ghomi, J. Raman Spectrosc. **45**, 657 (2014)
45. H.E. Van Wart, A. Lewis, H.A. Scheraga, F.D. Saeva, Proceedings of the National Academy of Sciences 70, 2619 (1973)
46. Z. Movasaghi, S. Rehman, I.U. Rehman, Appl. Spectrosc. Rev. **42**, 493 (2007)
47. W. Chen, H. Zhang, J. Wang, X. Hu, Chem. Nat. Compd. **55**, 461 (2019)
48. Y. Lu, P.-Y. Liu, P. Xiao, H.-W. Deng, Bioinformatics. **21**, 3105 (2005)
49. A. Polyakov, T. Alekseeva, I. Muravieva, in *E3S Web of Conferences*EDP Sciences, (2020), p. 01016
50. A. Yusuf, S.S. Fagbuaro, S.O.K. Fajemilehin, J. Biosci. Biotechnol. Discov. **3**, 105 (2018)
51. B.A. Akinwande, S.J. Olatunde, Int. Food Res. J. **22**, 332 (2015)

52. D. Dragolova, M. Dimitrova, M. Kouzmanova, in (Universitatea de Științe Agronomice și Medicină Veterinară București, București, 2009), pp. 317–329
53. K. Qian, C. Yao, Y. Wang, Q. Yang, S. Xiang, Q. Pei, T. Zhu, H. Liu, S. Dong, IEEE Trans. Biomed. Eng. **72**, 3233–3243 (2025)
54. F. Liu, Z. Wang, N. Yang, Y. Jin, X. Xu, Innovative Food Sci. Emerg. Technol. **109**, 104427 (2025)
55. J.R. Ferraro, *Introductory Raman Spectroscopy* (Elsevier, 2003)
56. D.A. Long, (No Title) (2002)
57. M. Zhang, Y. Wang, Q. Li, Y. Luo, L. Tao, D. Lai, Y. Zhang, L. Chu, Q. Shen, D. Liu, Heliyon 10, (2024)
58. A. Shang, S.-Y. Cao, X.-Y. Xu, R.-Y. Gan, G.-Y. Tang, H. Corke, V. Mavumengwana, H.-B. Li, Foods. **8**, 246 (2019)
59. R.J. Moses, G.I. Edo, A.N. Jikah, J.J. Agbo, Curr. Food Sci. Technol. Rep. **2**, 111 (2024)
60. J.Y. Ahn, D.Y. Kil, C. Kong, B.G. Kim, Asian-Australas J. Anim. Sci. **27**, 1615 (2014)
61. R. ElGamal, C. Song, A.M. Rayan, C. Liu, S. Al-Rejaie, G. ElMasry, Agronomy. **13**, 1580 (2023)
62. L. Zhang, S. Cao, J. Li, G. Wang, Foods. **11**, 2080 (2022)
63. M.A.S. Jiku, M. Alimuzzaman, A. Singha, M.A. Rahaman, R.K. Ganapati, M.A. Alam, S.R. Sinha, Bull. Natl. Res. Cent. **44**, 9 (2020)
64. M. Sustr, A. Soukup, E. Tylova, Plants. **8**, 435 (2019)
65. O.P. Narayan, P. Kumar, B. Yadav, M. Dua, A.K. Johri, Plant. Signal. Behav. **18**, 2030082 (2023)
66. A. Francioso, A. Baseggio Conrado, L. Mosca, M. Fontana, Oxid. Med. Cell. Longev. 2020, 8294158 (2020)